AJNR

Evaluation of cerebral perfusion from bypass arteries using selective intraarterial microsphere tracer after vascular reconstructive surgery.

I Nochide, S Ohta, T Ueda, M Shiraishi, H Watanabe, S Sakaki and J Ikezoe

Evaluation of Cerebral Perfusion from Bypass Arteries Using Selective Intraarterial Microsphere Tracer after Vascular Reconstructive Surgery

Ichiro Nochide, Shinsuke Ohta, Toshihiro Ueda, Masahiro Shiraishi, Hideaki Watanabe, Saburo Sakaki, and Junpei Ikezoe

BACKGROUND AND PURPOSE: To detect areas of cerebral perfusion from bypass arteries after vascular reconstruction, we administered selective intraarterial microsphere tracer into the external carotid arteries and determined (via single-photon emission computed tomography [IA-SPECT]) whether the distribution of radiotracer matched the arteriographic distribution of contrast material as shown on external carotid angiograms.

METHODS: We compared the extent of regional distribution of tracer after external carotid artery injection of 20 to 40 MBq of ^{99m}Tc-HMPAO or ^{99m}Tc-ECD with that of contrast medium on the external carotid angiograms in 582 cortical regions in 12 patients with atherosclerotic occlusive disease and in 18 patients with moyamoya disease.

RESULTS: Marked accumulation of tracer was found only in the expected, specific, newly developed areas of cerebral perfusion from bypass arteries. The regional distribution of tracer corresponded to that of contrast medium in 523 regions (90%) and did not correspond in 59 regions (10%). Significant overestimation of the distribution of contrast material relative to that of tracer was observed in the patients with moyamoya disease.

CONCLUSION: SPECT showed slightly different distribution of tracer from that predicted by conventional angiography. IA-SPECT should enhance the analysis of newly developed areas of cerebral perfusion from the bypass arteries.

To assess the usefulness of surgical vascular reconstruction, it is important to assess the blood supply to the areas of the brain covered by the bypass arteries, since it has been reported that improvement of cerebral blood flow (CBF) and postoperative clinical outcome were better in those patients with cerebral arterial occlusion who received wider postoperative perfusion from bypass arteries (1–5). When determining the contribution of vascular reconstruction to the improvement of CBF, specific identification of newly developed areas of cerebral perfusion from the bypass artery is essential, since any analysis of surgical outcome in patients with cerebrovascular occlusion must incorporate the postoperative blood-flow en-

hancement to these lesions. Perfusion studies with MR imaging or CT are limited to relatively large cerebral vessels, with neither technique able to adequately depict the capillary network (6). Angiographic evaluation of newly developed areas of perfusion from the bypass arteries is time-consuming and laborious in that, since the entire area of neovascularization is not displayed on the same angiogram, and since arteries do not always supply the brain tissue directly beneath them, careful observation of consecutive angiograms from the arterial to the venous phase is required. Moreover, Jeffery et al (7) have pointed out the risk of overestimating the distribution of contrast medium in the angiographic evaluation of the perfusion area of a specific artery relative to that supplied by natural blood flow, because both a faster injection rate and larger injection volume of contrast medium overcome the effects of laminar and contralateral flow. Therefore, an appropriate method is required for usefully and conveniently obtaining images in which the newly developed areas of cerebral perfusion from the bypass arteries can be instantly recognized.

^{99m}Tc-labeled hexamethylpropyleneamine oxime

(^{99m}Tc-HMPAO) and ^{99m}Tc-labeled ethylcysteinate dimer (^{99m}Tc-ECD) are radiolabeled substances with microspheric tracer characteristics that were developed for single-photon emission computed tomographic (SPECT) measurement of CBF. The major portion of each tracer enters the brain through functioning capillaries during the first pass through the circulation and is trapped at the extracted area for a relatively long time (8–11). Therefore, when one of the radiolabeled tracers is injected into a specific artery, a very high proportion of tracer remains in the area perfused by the artery and can be detected by SPECT. To depict newly developed areas of cerebral perfusion from the bypass arteries, we injected selective intraarterial ^{99m}Tc-HMPAO or ^{99m}Tc-ECD into the external carotid arteries in patients with arterial occlusive disease after vascular reconstructive surgery. ^{99m}Tc-ECD was used for most patients and ^{99m}Tc-HMPAO was used in a few earlier patients; ^{99m}Tc-labeled ECD has recently become available and is easier to prepare than ^{99m}Tc-HMPAO. Our purpose was to examine the appropriateness and convenience of this method by comparing the resulting distribution with that of contrast medium on conventional external carotid angiograms.

Methods

Subjects

We injected intraarterial microsphere tracer in 42 hemispheres of 30 patients who had undergone vascular reconstructive surgery. Thirty hemispheres of 18 patients with moyamoya disease (seven males and 11 females; mean age, 31 years; range, 8 to 57 years) (Table 1) were examined using intraarterial injection of microsphere tracer into the external carotid arteries after vascular reconstruction surgery. We used ^{99m}Tc-HMPAO as the tracer in three hemispheres of four patients and ^{99m}Tc-ECD in 27 hemispheres of 16 patients. The subtypes of the disease were adult moyamoya in 15 patients and childhood moyamoya in three patients. The initial onset patterns were intracerebral hemorrhage in three patients, intraventricular hemorrhage in four, subarachnoid hemorrhage in one, brain infarction in four, transient ischemic attack (TIA) in five, and incidental in one. Preoperative Suzuki's angiographic stages (12) were as follows: stage 1 in three hemispheres, stage 2 in six hemispheres, stage 3 in 17 hemispheres, and stage 4 in four hemispheres. In 18 hemispheres we performed direct anastomosis, such as superficial temporal artery (STA)-middle cerebral artery (MCA) anastomosis, primarily in the usual MCA and anterior cerebral artery (ACA) territories; in some, direct anastomosis was performed in combination with indirect anastomosis, including encephalomyosynangiosis (EMS) and/or encephalogaleosynangiosis (EGS); and in 12 hemispheres we performed indirect anastomosis alone, including encephaloduroarteriosynangiosis (EDAS), EMS, and/or EGS in the same territories. STA-MCA anastomosis surgically connected one or two branches of the STA to branches of the MCA in an end-to-side fashion. Indirect anastomosis was expected to produce spontaneous, very small arterial anastomoses or capillary networks between the brain surface and muscle or galeal flap through placement of the temporal muscle or galeal flap directly on the surface of the brain. This procedure covers a wider region of the brain than the STA-MCA procedure, although its success is a little less certain (13, 14).

In 12 hemispheres of 12 patients with atherosclerotic arterial occlusive disease (eight men and four women; mean age, 63 years; range, 42 to 74 years), we intraarterially injected ^{99m}Tc-HMPAO or ^{99m}Tc-ECD into the external carotid arteries after vascular reconstruction (Table 2). The initial onset patterns were brain infarction in five patients, TIA in four, intraventricular hemorrhage in one, and incidental in two. The diagnoses were MCA occlusion in six patients, internal carotid artery (ICA) occlusion in four, ICA stenosis in one, and tandem stenosis of the ICA and MCA in one. We performed STA-MCA single anastomosis in eight hemispheres and double anastomoses in four hemispheres.

Clinical outcome was evaluated 6 months after the operation and classified as 1) no further attack: ischemic or hemorrhagic attack was not observed during the 6 months; 2) no change: no new symptoms occurred in the patients who had no symptoms preoperatively; or 3) worsened: new symptoms appeared during the 6-month observation period.

Intraarterial Injection of Microsphere Tracer and SPECT (IA -and IA+IV-SPECT)

At follow-up angiography, performed after vascular reconstruction, 20 to 40 MBq of ^{99m}Tc-HMPAO or ^{99m}Tc-ECD was injected manually in a pulsatile fashion over a period of 1 minute through an angiographic infusion catheter inserted into the proximal portion of the external carotid artery. Approximately 30 minutes after intraarterial injection (after the completion of angiography), the patient underwent SPECT, which was performed with a four-head rotating gamma camera with a spatial resolution of 21.3 mm full width at half-maximum intensity and an intersection gap of 3 mm (IA-SPECT). Then, 800 MBq of the same tracer was injected through a brachial vein and SPECT was performed again 5 minutes later to identify the relationship between the distribution of tracer on the IA-SPECT scan and the background cerebral structure (IA+IV-SPECT) (Fig 1). In several patients, we reconstructed 3D images from IA-SPECT or IA+IV-SPECT data using a surface-rendering method with commercial software (Application Visualization System Medical Viewer; Advanced Visual Systems, Waltham, MA). In the 3D reconstruction, different colors were assigned to the area of cortical distribution of tracer on the IA-SPECT images and to the other parts of the brain depicted on the IA+IV-SPECT images in order to clearly reveal the cerebral area perfused by the bypass arteries.

Assessment of Regional Distribution of Tracer on IA-SPECT Images and of Regional Perfusion from Bypass Arteries on External Carotid Angiograms

Using 9-mm-thick transaxial IA-SPECT or IA+IV-SPECT images reconstructed on the basis of an orbitomeatal line with 6-mm gaps, one cerebral hemisphere was divided into 15 cortical regions of interest (ROIs) (Fig 2). Each region was classified into one of the following four grades according to the regional extent of distribution of tracer: grade 1, tracer distributed throughout the whole ROI; grade 2, tracer distributed throughout 50% to 99% of the ROI; grade 3, tracer distributed throughout less than 50% of the ROI; and grade 4, no distribution of tracer in the ROI (Fig 2).

Each cerebral hemisphere, depicted on the external carotid angiogram in the lateral view, was divided into 15 ROIs in the same manner as for IA-SPECT; that is, the 9-mm-thick ROIs (with a 6-mm gap between each section) were placed on the external carotid angiogram along the orbitomeatal line (Fig 3). These regions were also classified into the same four grades according to the regional percentage of distribution of contrast medium, and newly developed collateral arteries from the bypass arteries were identified by careful visual inspection of the consecutive angiograms from the arterial to venous phase by three neurosurgeons who were blinded to the SPECT data (Fig 3). We then examined the agreement of classification between the IA-SPECT images and the external carotid angiograms.

TABLE 1: Summary for 30 hemispheres of 18 patients with moyamoya disease

Patient	Age (y)/ Sex	Side of Hemisphere	Initial Onset Pattern	Preoperative Suzuki's Angiographic Stage	Vascular Reconstructive Surgery	Microsphere Tracer	Clinical Outcome
1	8/M	Right	Ischemic attack	3	EDAS, EMS	^{99m}Tc-ECD	No further attacks
		Left	No symptoms	3	STA-MCA, EMS	^{99m}Tc-ECD	No change
2	9/M	Left	Ischemic attack (TIA)	4	EDAS, EGS	^{99m}Tc-ECD	No change
3	11/F	Right	Ischemic attack (TIA)	3	EDAS, EGS	^{99m}Tc-ECD	No further attacks
4	19/F	Right	Ischemic attack (TIA)	1	EDAS, EGS	^{99m}Tc-ECD	No further attacks
		Left	No symptoms	1	EDAS, EGS	^{99m}Tc-ECD	No change
5	20/M	Left	Ischemic attack (TIA)	3	STA-MCA, EGS	^{99m}Tc-ECD	No change
6	25/F	Right	Intraventricular hemorrhage	3	STA-MCA	^{99m}Tc-ECD	No further attacks
		Left	No symptoms	3	EGS	^{99m}Tc-ECD	No change
7	26/M	Right	Intraventricular hemorrhage	4	STA-MCA	^{99m}Tc-ECD	No further attacks
		Left	No symptoms	4	STA-MCA	^{99m}Tc-ECD	No change
8	29/F	Right	Intracerebral hemorrhage	2	EDAS	^{99m}Tc-ECD	No further attacks
		Left	Ischemic attack (TIA)	1	STA-MCA	^{99m}Tc-ECD	No further attacks
9	30/F	Left	Intracerebral hemorrhage	2	EDAS	^{99m}Tc-HMPAO	No further attacks
		Right	No symptoms	4	EDAS	^{99m}Tc-HMPAO	No change
10	35/F	Right	Intraventricular hemorrhage	2	STA-MCA	^{99m}Tc-HMPAO	No further attacks
11	36/F	Right	Subarachnoid hemorrhage	3	STA-MCA	^{99m}Tc-ECD	No further attacks
		Left	No symptoms	3	STA-MCA, EMS	^{99m}Tc-ECD	No change
12	37/F	Left	Infarction	3	STA-MCA	^{99m}Tc-ECD	No further attacks
13	37/F	Right	Intracerebral hemorrhage	2	STA-MCA	^{99m}Tc-ECD	No further attacks
		Left	No symptoms	3	STA-MCA, EMS	^{99m}Tc-ECD	No change
14	37/F	Left	Infarction	3	STA-MCA	^{99m}Tc-ECD	No further attacks
		Right	No symptoms	2	STA-MCA, EMS	^{99m}Tc-ECD	No change
15	41/F	Right	Intraventricular hemorrhage	2	EDAS, EMS	^{99m}Tc-ECD	No further attacks
		Left	No symptoms	3	EDAS	^{99m}Tc-ECD	No change
16	47/M	Right	Ischemic attack (TIA)	3	STA-MCA, EMS, EGS	^{99m}Tc-ECD	No further attacks
		Left	No symptoms	3	STA-MCA, EMS, EGS	^{99m}Tc-ECD	No change
17	49/M	Right	Infarction	3	STA-MCA, EMS	^{99m}Tc-ECD	No further attacks
		Left	No symptoms	3	EDAS, EGS	^{99m}Tc-ECD	No change
18	57/M	Left	No symptoms	3	STA-MCA	^{99m}Tc-ECD	No change

Note.—TIA indicates transient ischemic attack; EDAS, encephaloduroarteriosynangiosis; STA-MCA, superficial temporal artery-middle cerebral artery anastomosis; EGS, encephalogaleosynangiosis; EMS, encephalomyosynangiosis; ^{99m}Tc-ECD, technetium-99m-labeled I,I-ethylcysteinate dimer; ^{99m}Tc-HMPAO, technetium-99m-labeled d,I-hexamethylpropyleneamine oxime.

Results

Representative Cases

Patient 16.—A 47-year-old man with headache and acute dizziness was found to have bilateral ICA obstruction with marked basal angiogenesis and collateral vessels (ie, moyamoya disease) at angiography. During vascular reconstruction in both hemispheres, the frontal and parietal branches of the STA were connected directly to the precentral and angular arteries in combination with EGS and EMS on both sides. IA-SPECT was performed at follow-up angiography 1 month after the surgery. On the right external angiograms, the collateral circulation to the MCA branches in the frontal lobe and the anterior part of the parietal lobe was observed mainly through the frontal branch of the STA-precentral arterial anasto-

mosis, while another anastomosis to the angular artery was less patent (Fig 4A). On the left side, both anastomoses were patent and the frontal and parietal branches, including a more posterior part of the parietal branches than on the right side, were depicted (Fig 4B). On the IA-SPECT images, a wide cortical distribution of tracer was evident on both sides, greater in the posterior part of the left side than the right side. The IA+IV-SPECT images showed the entire cerebral structure, and the area of tracer accumulation was of even greater intensity than on the IA-SPECT images (Fig 4C). The 3D images reconstructed from the IA-SPECT and IA+IV-SPECT scans clearly showed the area of cortical distribution of tracer injected into the external carotid arteries (Fig 4D).

Patient 23.—A 64-year-old man with loss of con-

TABLE 2: Summary for 12 hemispheres of 12 patients with atherosclerotic cerebral ischemic disease

Patient	Age (y)/ Sex	Diagnosis	Initial Onset Pattern	Donor Artery	Recipient Artery	Microsphere Tracer	Clinical Outcome
19	42/F	Right MCA occlusion	Ischemic attack (TIA)	STA parietal branch	Posterior temporal artery	99mTc-ECD	No further attacks
20	55/M	Left MCA occlusion	Infarction	STA parietal branch	Middle temporal artery	99mTc-ECD	No further attacks
21	58/M	Right ICA occlusion	Intraventricular hemorrhage	STA frontal branch STA parietal branch	Frontal ascending branch posterior temporal artery	99mTc-ECD	No further attacks
22	63/M	Right ICA stenosis, right MCA stenosis	No symptoms	STA parietal branch	Middle temporal artery	99mTc-ECD	No change
23	64/M	Right ICA stenosis	Ischemic attack (unstable)	STA frontal branch STA parietal branch	Precentral artery, middle temporal artery	99mTc-ECD	No further attacks
24	65/M	Left MCA occlusion	Ischemic attack (TIA)	STA parietal branch	Precentral artery	99mTc-HMPAO	No change
25	65/M	Right MCA occlusion	Infarction	STA frontal branch	Posterior temporal artery	99mTc-ECD	No further attacks
26	65/M	Right ICA occlusion	Infarction	STA parietal branch	Anterior parietal artery	99mTc-ECD	No further attacks
27	66/F	Right ICA occlusion	Ischemic attack (TIA)	STA parietal branch	Posterior temporal artery	99mTc-ECD	Worsened
28	70/F	Right MCA occlusion	Infarction	STA frontal branch STA parietal branch	Angular artery, middle temporal artery	99mTc-ECD	No further attacks
29	71/M	Right ICA occlusion	No symptoms	STA frontal branch STA parietal branch	Precentral artery, posterior temporal artery	99mTc-ECD	No change
30	74/F	Right MCA occlusion	Infarction	STA parietal branch	Precentral artery	99mTc-ECD	No further attacks

Note.—TIA indicates transient ischemic attack; MCA, middle cerebral artery; ICA; internal carotid artery; STA, superficial temporal artery; 99mTc-ECD, technetium-99m-labeled I,I-ethylcysteinate dimer; 99mTc-HMPAO: technetium-99m-labeled d,I-hexamethylpropyleneamine oxime.

Intra-arterial injection of 20-40 MBq of
99mTc-HMPAO or 99mTc-ECD
from the proximal portion of
external carotid artery
at time of angiography

↓ 30 min.

1st SPECT (IA SPECT)

↓

Intra-venous injection of 800 MBq of
99mTc-HMPAO or 99mTc-ECD
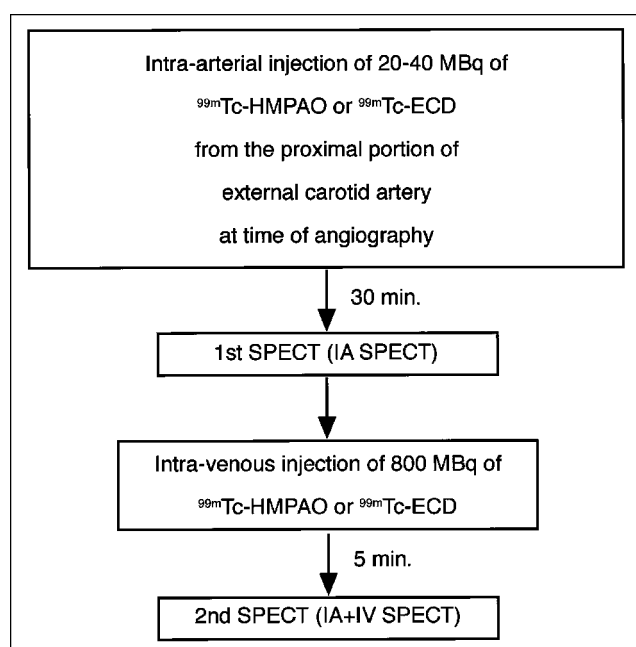
↓ 5 min.

2nd SPECT (IA+IV SPECT)

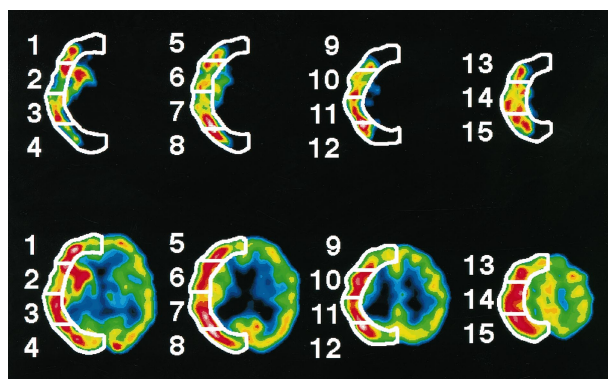FIG 1.   Protocol for IA-SPECT and IA+IV-SPECT.

FIG 2.   *Top row,*: IA-SPECT images. Note marked accumulation of tracer in part of the brain.

Bottom row, IA+IV-SPECT images allow identification of the cerebral structures and also show the area of marked accumulation of tracer seen on the IA-SPECT images. The transaxial IA+IV-SPECT images were reconstructed on the basis of the orbitomeatal line, wherein one cerebral hemisphere was divided into 15 cortical ROIs. The regional extent of tracer distribution was classified into four grades as described in the Methods section. Here, regions 2, 3, 6, 7, 10, 11, and 14 were classified as grade 1; region 15 was classified as grade 2; regions 1, 4, 5, 8, 9, 12, and 13 were classified as grade 3; and no region was classified as grade 4.
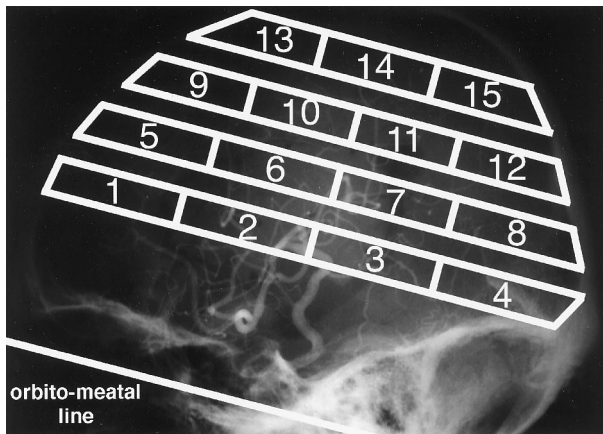
FIG 3.   On this lateral-view external carotid angiogram, we divided the cerebral hemisphere into 15 regions, and then classified the regions into four grades according to the extent of distribution of contrast medium from the arterial to venous phase in the same manner as for the IA-SPECT images.

sciousness and acute left-sided hemiparesis was found to have severe (95%) and long segmental atherosclerotic stenosis at the right carotid siphon at cerebral angiography. During emergency surgery, the right frontal branch of the STA was connected directly to the precentral artery, and the parietal branch was connected to the middle temporal artery. Angiography and IA-SPECT and IA+IV-SPECT were performed 40 days after the STA-MCA anastomosis. Marked accumulation of ^{99m}Tc-ECD was observed in the part of the brain in which there was no depiction of background on the IA-SPECT images. The IA+IV-SPECT images showed the accumulation of tracer observed on the IA-SPECT images distributed in the frontal, parietal, and temporal lobes, the insula, and the lentiform nucleus (Fig 5A). These tracer distributions corresponded to the findings of external carotid angiography, which showed the MCA branches in the frontal, parietal, and temporal lobes and the perforating arteries from the M1 portion (Fig 5B and C).
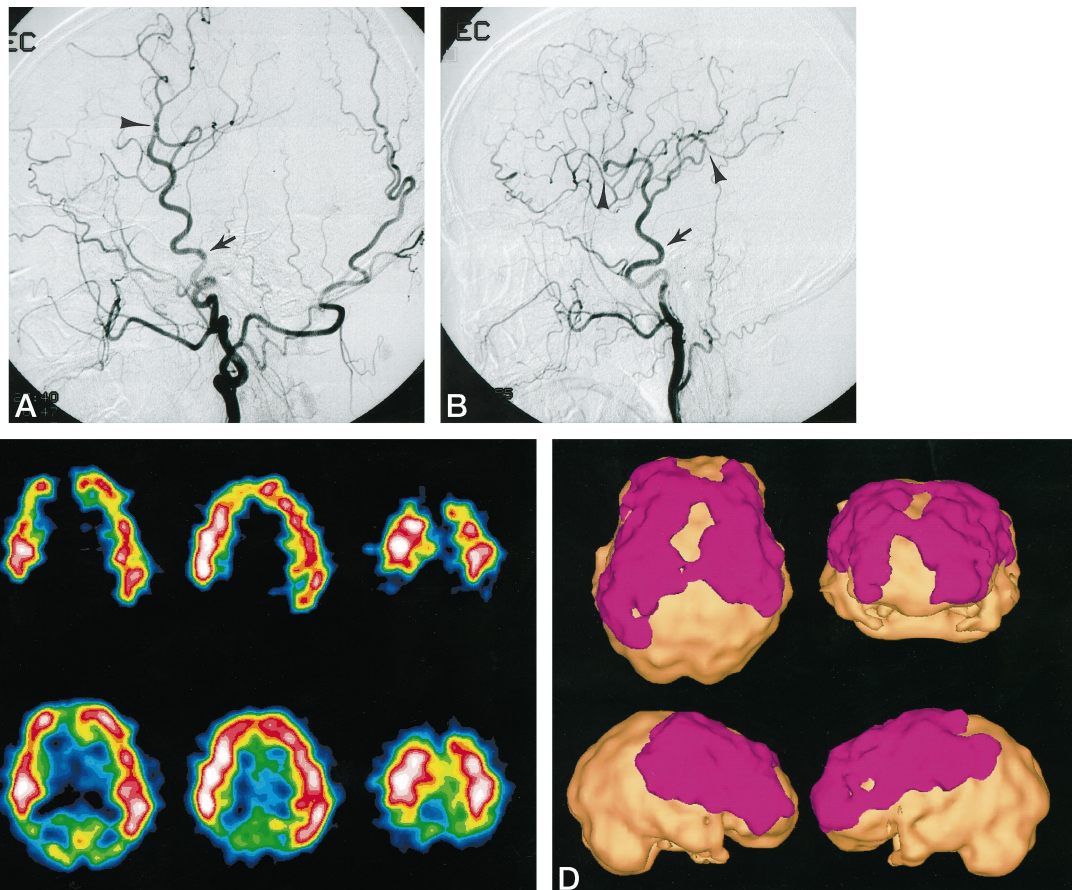

FIG 4.   Patient 16.

A and *B*, External carotid angiograms. On the right side (*A*), the collateral circulation to the MCA branches in the frontal lobe and the anterior part of the parietal lobe is observed mainly through the frontal branch of the STA (*arrow*). *Arrowhead* indicates precentral arterial anastomosis. On the left side (*B*), the frontal and parietal branches, including a more posterior part of the parietal branches than on the right side, are depicted (*arrow*). Both anastomoses are patent (*arrowheads*).

C, IA-SPECT and IA+IV-images. On the IA-SPECT images (*top row*), wide cortical distribution of the tracer is seen on both sides; in the posterior part, distribution is wider on the left than on the right. The IA+IV-SPECT images (*bottom row*) show location of areas of marked accumulation on the IA-SPECT images.

D, Three-dimensional images reconstructed from the IA-SPECT and IA+IV-SPECT images by the surface-rendering method. The area of cortical distribution of the tracer is assigned the color purple; the other parts of the brain are peach colored. These images clearly depict the surface of the newly developed area perfused from the bypass arteries after vascular reconstructive surgery.
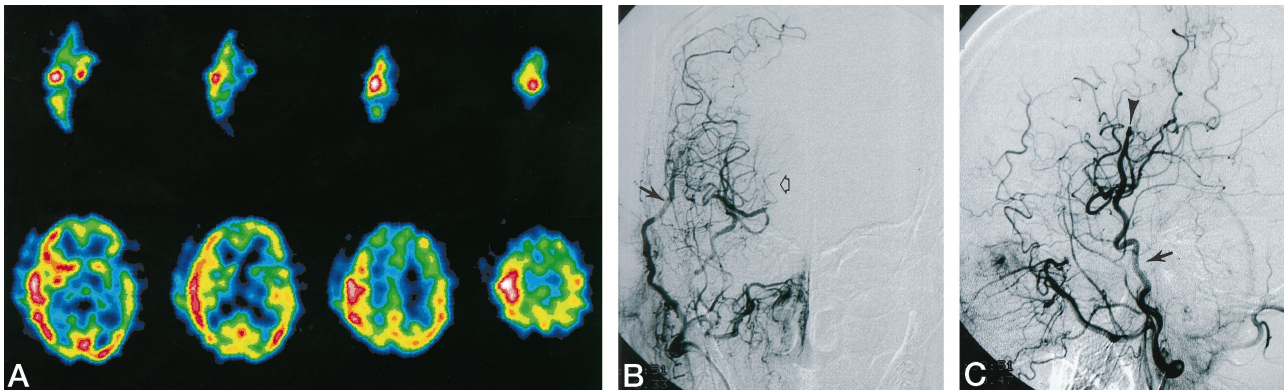
Fig 5.   Patient 23.
A, IA-SPECT (*top row*) and IA+IV-SPECT (*bottom row*) images with ^{99m}Tc-ECD tracer 40 days after right-sided STA-MCA anastomosis. Marked accumulation of ^{99m}Tc-ECD (in the frontal, parietal, and temporal lobes, the insula, and the lentiform nucleus) is clearly depicted in the portion of the right brain that does not show background on the IA-SPECT images. The finding of newly developed cerebral perfusion from the STA on the IA-SPECT images is well corroborated by the external carotid angiograms.
B and *C*, Right external carotid angiogram, on which the MCA branches in the frontal, parietal, and temporal lobes and the perforating arteries (*open arrow*) from the M1 portion are depicted from the right frontal branch of the STA (*solid arrow*). *Open arrow* indicates precentral artery anastomosis.

Clinical Outcome

Among patients with moyamoya disease, 16 hemispheres had no further ischemic or hemorrhagic attacks during the 6 months after vascular reconstruction; before reconstruction, eight hemispheres had ischemic and eight had hemorrhagic attacks. Two patients had TIAs postoperatively, and no patient experienced worsening of symptoms. Among patients with atherosclerosis, eight had no further TIA during the 6-month observation, one had a TIA postoperatively, and one had new symptoms postoperatively caused by a subdural hematoma.

Comparison of IA-SPECT and Angiographic Findings

Among patients with moyamoya disease, excluding 26 apparent infarct regions, 424 regions were examined. In 368 regions (87%), classification of the regional distribution of ^{99m}Tc-HMPAO or ^{99m}Tc-ECD injected into the external carotid artery corresponded to the regional classification determined from the external carotid arteriograms. The regional distribution of tracers was more narrow than that of contrast medium on the angiogram in 20 regions (5%), and was wider in 36 regions (8.5%) (Table 3, upper portion). In the patients with atherosclerotic cerebral ischemic disease, 158 regions were examined after exclusion of 22 apparent infarct regions. In 155 regions (98%), classification of the regional distribution of ^{99m}Tc-HMPAO or ^{99m}Tc-ECD on the IA-SPECT images corresponded to the angiographic classification. Only three regions (2%) showed a difference in the regional classification between the IA-SPECT images and the angiograms (Table 3, middle portion). Both in patients with moyamoya disease and atherosclerotic disease, all the regions considered to be perfused by the bypass arteries showed tracer distribution, and no region without tracer distribution was found among the regions with such perfusion (Table 3, lower portion). However, in the mismatched regions, a significant difference was noted in the patients with moyamoya disease. The distribution of contrast medium was significantly overestimated on the conventional external carotid angiograms as compared with the distribution of tracer on the IA-SPECT images (signed test, $P < .05$).

Discussion

Several of the tracers developed to measure CBF with the use of SPECT have, to some extent, been based on microsphere characteristics, in which the delivery and entrance of the tracer to the brain depend only on blood flow; back-flux from the brain to blood is negligible, and the tracer is trapped in the brain for a prolonged time. Making use of these characteristics, we evaluated the area of the brain perfused by a specific artery using selective intraarterial injection of ^{99m}Tc-HMPAO and ^{99m}Tc-ECD. When performing the IA-SPECT protocol, we estimated that the optimal amount of ^{99m}Tc-HMPAO or ^{99m}Tc-ECD for IA-SPECT was 20 to 40 MBq based on a report that approximately 5% of the total dose of administered ^{99m}Tc-HMPAO is accumulated in brain tissue on conventional SPECT scans when 1110 MBq is administered intravenously. We chose a slow, manual, and pulsatile method of intraarterial administration of the tracers, since it has been reported that such a method may minimize the laminar effect in the injected vessels, mix the tracer with blood, and deliver the tracer to tissue capillaries, which is more consistent with natural blood flow, as the tracer is evenly distributed in the vessels into which it is being injected (15–18). Therefore, we considered that the tracer injected into the external carotid artery in this procedure flows in the physiological bloodstream. We injected the tracer from the proximal portion of the external carotid artery because the many branches arising from this artery, such

TABLE 3: Cerebral distribution (number of regions) of ^{99m}Tc-HMPAO or ^{99m}Tc-ECD as compared with the distribution of contrast medium on external carotid angiograms

Grade of Distribution of ^{99m}Tc-HMPAO or ^{99m}Tc-ECD		Grade of Distribution of Contrast Medium				Total
		1	2	3	4	
Moyamoya disease						
	1	24	14	0	0	38
	2	12	75	3	0	90
	3	0	14	74	3	91
	4	0	0	10	195	205
	Total	36	103	87	198	424
Atherosclerotic arterial occlusive disease						
		50	1	0	0	51
		0	47	0	0	47
		0	1	36	1	38
		0	0	0	22	22
	Total	50	49	36	23	158
Total regions for moyamoya and atherosclerotic disease						
		74	15	0	0	89
		12	122	3	0	137
		0	15	110	4	129
		0	0	10	217	227
	Total	86	152	123	221	582

Note.—Grade 1 indicates 100% perfusion from the bypass artery; grade 2, 99% to 50% perfusion from the bypass artery; grade 3, 49% to 1% perfusion from the bypass artery; grade 4, 0% perfusion from the bypass artery.

as the middle and deep temporal arteries, together with the STA, participate in the development of collateral circulation to the brain after EMS and/or EGS surgery in patients with moyamoya disease.

Strictly speaking, ^{99m}Tc-HMPAO and ^{99m}Tc-ECD are not ideal microsphere tracers because their first-pass extraction fractions from the blood to the brain are estimated to be approximately 80% and 70%, respectively. That is, both show relatively low extraction fractions compared with those of perfect microsphere tracers. After entry into the brain parenchyma, the majority of ^{99m}Tc-HMPAO is immediately converted from lipid soluble to hydrophilic compounds, and ^{99m}Tc-ECD is deesterified to a metabolite that cannot pass through the blood-brain barrier. The portion of ^{99m}Tc-HMPAO and ^{99m}Tc-ECD that is not converted effluxes out from the brain parenchyma to the bloodstream again. Once trapped in the brain, however, ^{99m}Tc-HMPAO and ^{99m}Tc-ECD can be stable in the extracted area for a prolonged time, and the flow-dependent cerebral distribution of tracers at the time of injection may be detected later by SPECT, even if the CBF was altered after injection (8–11). The drawbacks inherent in the use of ^{99m}Tc-HMPAO and ^{99m}Tc-ECD as microsphere tracers may not have adversely affected the IA-SPECT study, because a very high percentage of the tracers was extracted only in the area perfused during the first pass, and the nonextracted portion passing through the brain or the

back-fluxed tracers from the brain to the blood might have been diluted to a negligible level during the subsequent systemic circulation. This technique enhances the microspheric character of the tracer, since recirculation of tracer can be considered excluded, and the actual IA-SPECT images showed only the portion of brain in which background was not evident, and therefore not indicative of the effect of recirculated tracer. Because ^{99m}Tc-ECD, after preparation, is more resistant to in vitro degeneration than ^{99m}Tc-HMPAO, we mainly used ^{99m}Tc-ECD once this tracer became available.

The IA-SPECT images appeared to lack sufficient anatomic information about the distribution of tracer, and thus it was difficult to locate the area of greatest accumulation by using these images alone. For this reason, we also administered the tracer intravenously at relatively low doses after IA-SPECT examination, and the IA+IV-SPECT images provided anatomic information for the entire brain without missing the marked accumulation of tracer observed on the IA-SPECT images after intraarterial injection. We reconstructed 3D images for several patients by using the IA+IV-SPECT images or a combination of IA-SPECT images. The reconstructed 3D images showed the cortical tracer distribution and indicated clearly where the perfusion from the bypass arteries developed, even though the spatial resolution of these images was poor. Merging of the IA-SPECT and MR

images could thus be expected to provide a clear picture of the perfusion area of the bypass arteries, indicating the precise anatomic location of the distribution of tracer.

We compared the regional extent of distribution of tracer on the IA-SPECT images with that of contrast medium from the bypass arteries estimated from the serial external carotid angiograms. To compare the cerebral distribution of tracer on IA-SPECT images and contrast medium on external angiograms, we divided one hemisphere into 15 ROIs, and the distribution of tracer or contrast medium in each region was globally divided into four grades. We adopted a global estimation for the following reasons. The ROIs of the IA-SPECT images were not completely matched to those of the angiograms, because the cranium was curved and the horizontal outline of the ROI was nonlinear on the IA-SPECT image and linear on the angiogram, even though the vertical planes of the two techniques were completely matched. Moreover, conventional angiography requires a larger volume of contrast medium and a higher injection pressure and speed, which cause a disturbance in the natural blood flow in vessels, thereby eliminating the laminar flow effect or employing vessels with contralateral and collateral flow. This ultimately risks a wider distribution of contrast medium than of tracer for IA-SPECT, which is more dependent on natural blood flow. Although the present comparison included a number of potentially mismatching factors, it was hoped that the global grading estimates would show some correlation, and, indeed, very good correlations were found. However, there was a significant overestimation of the distribution of contrast medium as compared with that of tracer on IA-SPECT images in patients with moyamoya disease. We think this difference was due to the more complicated spatial cerebral circulation and longer circulation time from the bypass arteries in patients with moyamoya disease relative to those with atherosclerosis. Many more transdural and transarterial anastomoses (such as middle meningeal artery, temporal muscle, and galeal branches other than STA) were developed as anastomoses in the patients with moyamoya disease, and the effects of disturbance of the natural blood flow on conventional angiograms might have been greater than those in the patients with atherosclerosis. We believe that the IA-SPECT method covered a more reasonable and appropriate cerebral area of perfusion from the bypass arteries than did conventional angiography, because tracer delivery was more natural, as mentioned above.

Conclusion

Unfortunately, the absolute volume of blood flow from the bypass arteries cannot be determined at present, owing to a lack of knowledge of the arterial time-activity changes of the tracer in the injected (external carotid) artery. We conclude that IA-SPECT is a useful technique for providing appropriate images as a result of a tracer delivery method that is more dependent on natural blood flow. This technique should enhance the analysis of newly developed areas of cerebral perfusion from bypass arteries in patients who have undergone vascular reconstruction.

References

1. Bradac GB, Schramm J, Kaernbach A, Oppel F. **Angiographic aspects of extra- intracranial arterial bypass for cerebral arterial occlusive disease.** *Neuroradiology* 1980;20:111–122
2. Anderson RE, Reichman OH, Davis DO. **Radiological evaluation of temporal artery-middle cerebral artery anastomosis.** *Radiology* 1974;113:73–79
3. Latchaw RE, Ausman JI, Lee MC. **Superficial temporal-middle cerebral artery bypass: a detailed analysis of multiple pre- and postoperative angiograms in 40 consecutive patients.** *J Neurosurg* 1979;51:455–465
4. Nariai T, Suzuki R, Matsumura Y, et al. **Surgically induced angiogenesis to compensate for hemodynamic cerebral ischemia.** *Stroke* 1994;25:1014–1021
5. Schmiedek P, Piepgras A, Leinsinger G, Kirsch CM, Einhaupl K. **Improvement of cerebrovascular reserve capacity by EC-IC arterial bypass surgery in patients with ICA occlusion and hemodynamic cerebral ischemia.** *J Neurosurg* 1994;81:236–244
6. Bihan DL, Breton E, Lallemand D, Grenier P, Cabanis E, Jeantet ML. **MR imaging of intravoxel incoherent motions: application to diffusion and perfusion in neurologic disorders.** *Radiology* 1986;161:401–407
7. Jeffery PJ, Monsein LH, Szabo Z, et al. **Mapping the distribution of amobarbital sodium in the intracarotid Wada test by use of Tc-99m HMPAO with SPECT.** *Radiology* 1991;178:847–850
8. Anderson AR, Friberg HH, Schmidt JF, Hasselbalch SG. **Quantitative measurements of cerebral blood flow using SPECT and [99mTc]-d,l-HM-PAO compared to Xe-133.** *J Cereb Blood Flow Metab* 1988;8:S69–S81
9. Leonald J, Nowotnik DP, Neirinckx RD. **Technetium-99m-d,l-HM-PAO, a new radiopharmaceutical for imaging regional brain perfusion using SPECT: a comparison with iodine-123 HIPDM.** *J Nucl Med* 1986;27:1819–1823
10. Neirinckx RD, Canning LR, Piper IM, et al. **Technetium-99m d,l-HM-PAO: a new radiopharmaceutical for SPECT imaging of regional cerebral blood-perfusion.** *J Nucl Med* 1987;28:191–202
11. Walovitch R, Hill T, Garrity S, et al. **Characterization of technetium-99m-l,l-ECD for brain perfusion imaging, 1: pharmacology of technetium-99m ECD in nonhuman primates.** *J Nucl Med* 1989;30:1892–1901
12. Suzuki J, Takaku A. **Cerebrovascular "moyamoya" disease.** *Arch Neurol* 1969;20:288–299
13. Karasawa J, Kikuchi H, Furuse S, et al. **A surgical treatment of "moyamoya" disease "encephalo-myo synangiosis."** *Neurol Med Chir (Tokyo)* 1977;17:29–37
14. Matsushima Y, Inaba Y. **Moyamoya disease in children and its surgical treatment: introduction of a new surgical procedure and its follow-up angiograms.** *Childs Brain* 1984;11:155–170
15. Lutz RJ, Dedrick RL, Boretos JW, Oldfield EH, Blacklock JB, Doppman JL. **Mixing studies during intracarotid artery infusions in an in vitro model.** *J Neurosurg* 1986;64:277–283
16. Saris SC, Shook DR, Blasberg RG, et al. **Carotid artery mixing with diastole-phased pulsed drug infusion.** *J Neurosurg* 1987;67:721–725
17. Shook DR, Beaudet BS, Doppman JL. **Uniformity of intracarotid drug distribution with diastole-phased pulsed infusion.** *J Neurosurg* 1987;67:726–731
18. Aoki S, Terada H, Kosuda S. **Supraophthalmic chemotherapy with long tapered catheter: distribution evaluated with intraarterial and intravenous Tc-99m HMPAO.** *Radiology* 1993;188:347–350